

TITLE PAGE

Citation Format:

S. K. V. Sekar, A. Farina, E. Martinenghi, A. Dalla Mora, P. Taroni, A. Pifferi, E. Negro, J. Puig, R. Escrig, Q. Rosales, C. Lindner, M. Pagliazzi, and T. Durduran, "Time-resolved diffused optical characterization of key tissue constituents of human bony prominence locations," in *DIFFUSE OPTICAL IMAGING V*, P. Dehghani, H and Taroni, ed., Proceedings of SPIE (SPIE-INT SOC OPTICAL ENGINEERING, 2015), Vol. 9538.

Copyright notice:

Copyright 2015 Society of Photo-Optical Instrumentation Engineers. One print or electronic copy may be made for personal use only. Systematic reproduction and distribution, duplication of any material in this paper for a fee or for commercial purposes, or modification of the content of the paper are prohibited.

DOI abstract link:

<http://dx.doi.org/10.1117/12.2183724>

Time-resolved diffused optical characterization of key tissue constituents of human bony prominence locations

Sanathana Konugolu Venkata Sekar¹, Andrea Farina¹, Edoardo Martinenghi¹, Alberto Dalla Mora¹, Paola Taroni¹, Antonio Pifferi^{1,2}, Eugènia Negrodo³, Jordi Puig³, Roser Escrig³, Quim Rosales⁴, Claus Lindner⁵, Marco Pagliazzi⁵, Turgut Durduran⁵

¹Politecnico di Milano, Dipartimento di Fisica, Milano, Italy; ²Consiglio Nazionale delle Ricerche, Istituto di Fotonica e Nanotecnologie, Milano, Italy; ³Fundació Lluita contra la SIDA, Hospital Germans Trias i Pujol, Badalona (Barcelona), Spain; ⁴Digest Centre Mèdic, Badalona (Barcelona), Spain; ⁵ICFO-Institut de Ciències Fotòniques,(Barcelona), Spain;

ABSTRACT

We report a broadband time-resolved characterization of selected bony prominence locations of the human body. A clinical study was performed at six different bony prominence locations of 53 subjects. A portable broadband time-resolved system equipped with pulse drift and distortion compensation strategy was used for absorption and scattering measurements. Key tissue constituents were quantified as a pilot step towards non-invasive optical assessment of bone pathologies.

Keywords: time-resolved spectroscopy, scattering, absorption, osteoporosis, bone, calcaneus, in-vivo, biomedical.

1. INTRODUCTION

Bone is subject to continuous change in response to loading caused by our daily activities. Remolding and damage caused by loading affect tissue composition¹. Non-invasive observation of physiological conditions of bone can predict pathologies related to bone. Classification of human and mammal bone is made on the bases of its porosity and microstructure² and it is of two types. The first dense cortical bone with porosity 5% to 10% is termed compact bone is commonly found in the shaft of long bones. The second spongy, more porous (50% to 90%) bone is termed trabecular or spongy bone. It is commonly found at the extremities of long bones or in flat bones as for example the pelvis or the sternum.

Dual X-ray Absorptiometry (DEXA) scan³ is applied on trabecular bone and is the gold standard to assess bone mineral density (BMD). The T-score is also used to characterize bone constitution. It is given by DEXA scans and can assess age independent degradation of bone. T-score of -1 to -2.5 and below -2.5 corresponds to osteopenia and osteoporosis conditions, respectively⁴. However, DEXA suffers from the invasiveness caused by the use of ionizing radiation. Ultrasound based techniques provide mainly structural and morphological information, but fail in judging precisely the physiological status of the bone⁵. Several other tests like x-ray scattering⁶ methods or Magnetic Resonance Imaging (MRI) based bone mineral discrimination have been reported, but all show limitations that prevent wide and effective application.

Previously, diffuse optical techniques were used to characterize bone tissue⁷. In reference to the problem of osteoporosis, interesting results were reported by light scattering techniques showing correlation between osteoporosis and bone scattering coefficient⁸. Preliminary in vivo optical measurements on 5 volunteers done on calcaneous bone⁹ showed interesting correlation between age, various tissue constituents (lipid, collagen, hemoglobin) and the scattering coefficient using a time-resolved broadband laboratory-based system¹⁰. Bone fibrous tissue structure consists of connective tissue, proteins (mostly collagen) and blood cells as major components. The concentration of collagen and other tissue constituents could be related to bone physiological condition and to alterations induced by pathologic conditions.

In our current work, we used a time-resolved diffused optical technique to measure in vivo broadband (600-1200 nm) optical properties in 6 different locations of 53 subjects. As the pathological changes are revealed early in the trabecular bones, we choose the distal and proximal extremities of ulna and radius in the arm trochanter in reflectance and calcaneous in transmittance for our studies. All these locations except the calcaneous were scanned with DEXA.

2. MATERIALS AND METHODS

2.1 System setup

A schematic diagram depicting the optical chain of the portable time-resolved system is shown in Fig. 1. The source is provided by a photonic crystal based supercontinuum fiber laser (SC450, Fianium, UK) with 6 W overall power over a spectral range 450-1750 nm. The pulses of width of few picoseconds are generated at a 40 MHz repetition rate. Spectral tunability is achieved by dispersing the source with a Pellin-Broca prism and coupling the selected wavelength into an optical fiber. To achieve higher responsivity, two different detectors, a Hamamatsu Silicon Photomultiplier (SiPM) possessing better temporal resolution (133 ps) than the previously reported SiPM detector based time resolved in vivo study¹¹ and Hamamatsu InGaAs PMT, are used over their corresponding efficient spectral regions. A pellicle beam splitter is used to change detector at desired wavelength. The system was designed to work efficiently over the range of 600-1200 nm. A reference line acquiring the instrument response function (IRF) synchronously with the signal is added with delay to optical chain to compensate for shape distortion in real time in a clinical environment. The probe consists of two slots to fix source and detector fibers and detachable foam, which is sterilized before each measurement. Reflectance measurements were done at 2.5 cm as source detector separation.

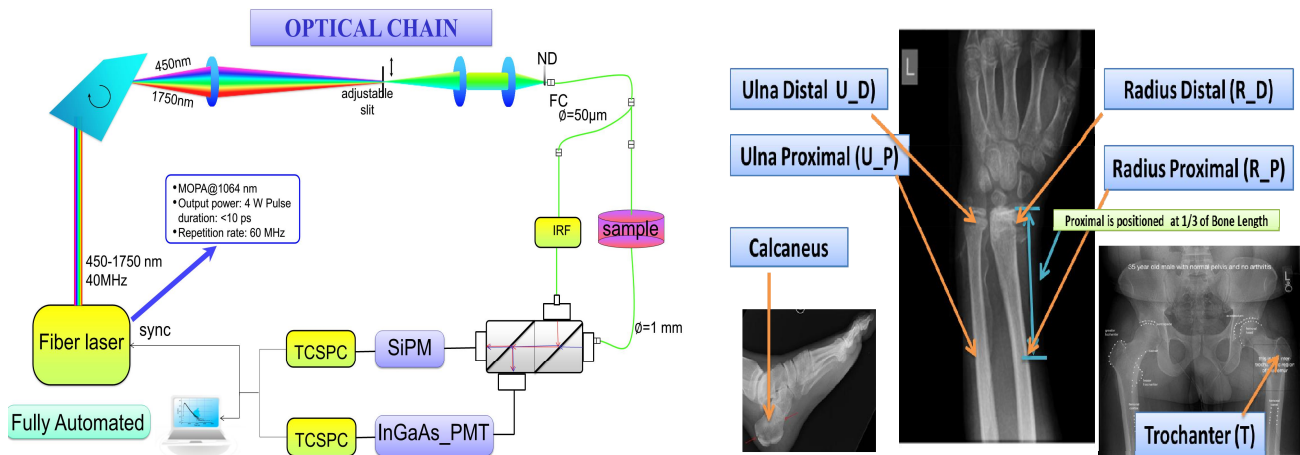


Fig. 1: Block diagram of system used in measurement (left) and bone prominence locations measured in the protocol (right)

2.2 Measurement Protocol

The study population consists of 53 subjects distributed over the age of 20 to 78 years, who were enrolled into the protocol with signed informed consent. The subjects were asked to fill in a basic health questionnaire regarding their history of anemia, lung disease, coronary artery disease, smoking etc. Blood pressure, oxygen saturation and pulse rate were measured before and after the optical measurement, ensuring an overall healthy condition for the subjects. Measurements at radius distal, radius proximal, ulna distal, ulna proximal were done by keeping the subject's hand in a comfortable position. For the trochanter location, measurements were performed by asking subjects to stand up and to lean gently on the ipsilateral side to expose further the bone. A customized probe ensuring a perfect transmittance geometry was used for calcaneus measurement. DEXA scans were taken for each subject in all locations except for the calcaneus.

3. DATA ANALYSIS

3.1 Evaluation of time-resolved optical data

Absorption (μ_a) and reduced scattering (μ'_s) coefficients were estimated by fitting experimentally acquired curves at each wavelength with an analytical solution of the diffusion approximation to the transport equation for a homogeneous semi-infinite medium or an infinite slab¹². Extrapolated boundary conditions were used. Theoretically predicted curves were convolved with acquired IRF and normalized to the experimentally acquired curve. 80% of peak value on the rising edge of the curve and 1% on the tail were chosen as the limits of the fitting range¹³.

3.2 Secondary fit

The percentage quantification of the key tissue constituents was performed by fitting the absorption spectra with a linear combination of the main tissue constituents (lipid, water, collagen, oxy-hemoglobin, deoxy-hemoglobin) spectra¹⁴. The absorption coefficient at each wavelength is given by the equation:

$$\mu_a(\lambda) = \sum_i c_i \varepsilon_i(\lambda)$$

where λ is the wavelength of light, c_i and ε_i are the concentration (free fit parameter) and the specific absorption of the i^{th} component, respectively.

The wavelength dependence of the scattering spectra can be approximated by a power law derived empirically from the Mie theory¹⁵ as:

$$\mu_s = a(\lambda/\lambda_0)^{-b}$$

for a certain fixed wavelength λ_0 . The exponent b is related to the mean effective size of scattering centers, while the amplitude a is related to the density of the scattering centers⁸.

4. RESULTS AND CONCLUSION

Figure 2 shows the sample broadband absorption spectra of a subject at the 6 different locations measured in the protocol. The solid line displays the absorption of the linear combination of key tissue constituents estimated by the secondary fitting procedure, while the dots are the broadband absorption values extracted by the diffusion model. The estimated absorption properties can vary significantly from case to case both at short wavelengths (where blood absorption is dominant) and on the absorption peaks of lipids at 930 nm and water around 980 nm.

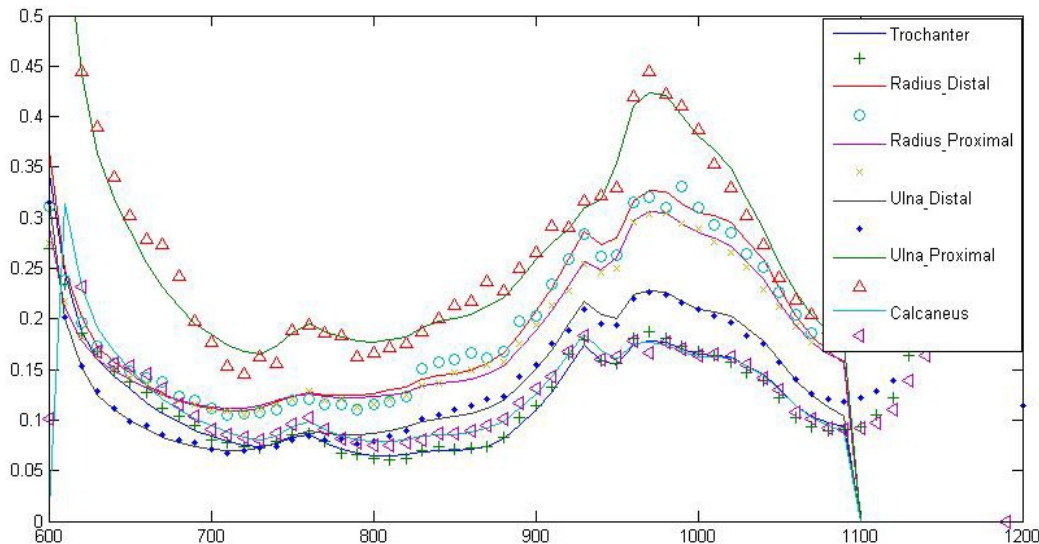


Figure 2: Broadband absorption spectra of 6 locations measured in the protocol.

Table 1 gives the quantified values of tissue constituents (lipid, water, collagen, oxy-,deoxy-hemoglobin, abbreviated HbO2 and Hb), total hemoglobin concentration (tHb) and tissue oxygen saturation (StO2) at the 6 locations.

In summary, time-resolved broadband measurements were performed on 53 subjects at 6 different bone prominence locations. The measured curves were primarily fitted for absorption values followed by a secondary fit to extract key tissue constituents. The plots depicting the fit to measured absorption values were plotted. The percentage key tissue constituents (water, lipid, collagen), oxy-,deoxy-hemoglobin (μM) along with scattering a and b values were tabulated in a Table 1. Our future goal is to investigate the correlation of the tissue constituents data with the gold standard DEXA

data to explore the feasibility of using time-resolved diffuse optics as a tool for assessing bone related pathologies. Also, bone marrow oxygenation and perfusion could be monitored¹⁶ in relation to physiological or pathological processes.

Table 1: Quantified values of tissue constituents at the 6 locations

Location	Hb [uM]	HbO2 [uM]	Lipid [%]	H2O [%]	Collagen [%]	Background [cm-1]	tHb [uM]	StO2 [%]	a [cm-1]	b
Trochanter	7.9	9.7	60.8%	21.9%	17.4%	0.00	17.7	55%	10.4	0.5
Radius Distal	0.6	27.7	55.8%	25.7%	18.5%	0.03	28.3	98%	8.3	0.6
Radius Proximal	0.3	18.9	54.4%	28.5%	17.1%	0.05	19.2	98%	8.4	0.5
Ulna Distal	2.2	23.1	65.1%	22.9%	12.0%	0.01	25.3	91%	3.8	1.3
Ulna Proximal	13.5	38.6	26.8%	42.7%	30.5%	0.02	52.0	74%	4.9	0.9
Calcaneous	9.5	11.0	68.3%	20.1%	11.6%	0.02	20.5	54%	11.7	0.4

ACKNOWLEDGMENTS

The research leading to these results has partially received funding from the EC's Seventh Framework Programme under the projects LASERLAB-EUROPE (grant agreement n. 284464,) and OILTEBIA (grant agreement n. 317526), Fundacio Cellex Barcelona, Marie Curie IRG (FP7, RTPAMON), Ministerio de Economia y Competitividad (PHOTOSTROKE), Obra Social La Caixa (LlumMedBCN), LASERLAB- EUROPE III (BIOPHTICAL).

REFERENCES

1. S. Gamsjäger et al., "Raman application in bone imaging," in Raman Spectroscopy for Soft Matter Applications, pp. 225–267, John Wiley & Sons, Inc., Hoboken, New Jersey (2009).
2. World Health Organization, "Assessment of fracture risk and its application to screening for postmenopausal osteoporosis: report of aWHO study group," World Health Org. Tech. Rep. Ser.843, 1–129(1994).
3. Mishra, Mahavir B; Mishra, Shanu; Mishra, Ranu (2011). "Dental Care in the Patients with Bisphosphonates Therapy". International Journal of Dental Clinics 3 (1): 60–4.
4. Y. Lu, H. K. Genant, J. Shepherd, S. Zhao, A. Mathur, T. P. Fuerst, and S. R. Cummings, "Classification of osteoporosis based on bone mineral densities," J. Bone Miner. Res.16, 901–910 (2001).
5. D. C. Bauer, C. C. Gluer, J. A. Cauley, T. M. Vogt, K. E. Ensrud, H.K. Genant, and D. M. Black, "Broadband ultrasound attenuation predicts fractures strongly and independently of densitometry in olderwomen. A prospective study of osteoporotic fractures group," Arch. Intern. Med.157, 629– 634 (1997)
6. American Medical Association, "Managing osteoporosis part 1: detection and clinical issues in testing," ~<http://www.ama-assn.org/cmeselec>
7. Farzam P, et al. , "Noninvasive characterization of the healthy human manubrium using diffuse optical spectroscopies", Physiol Meas 35, 1469-1491 (2014).
8. S. Majumdar, P. Augat, J. C. Lin, D. Newitt, Y. Lu, N. E. Lane, and H. K. Genant, "In vivo high-resolution MRI of the calcaneus: differences in trabecular structure in osteoporosis patients," J. Bone Miner. Res.13, 1175–1182 (1998).
9. A. Pifferi, A. Torricelli, P. Taroni, A. Bassi, E. Chikoidze, E. Giambattistelli, and R. Cubeddu, "Optical biopsy of bone tissue: a step toward the diagnosis of bone pathologies," J. Biomed. Opt. 9(3), 474–479 (2004).

10. Pifferi, A., Torricelli, A., Taroni, P., Comelli, D., Bassi, A., Cubeddu, R. Fully automated time domain spectrometer for the absorption and scattering characterization of diffusive media (2007) *Review of Scientific Instruments*, 78 (5), art. no. 053103.
11. Shin-ichi Fujisaka, Takeo Ozaki, Tsuyoshi Suzuki, Tsuyoshi Kamada, Ken Kitazawa, Mitsunori Nishizawa, Akira Takahashi and Susumu Suzuki "Clinical Tissue Oximeter using NIR Time-Resolved Spectroscopy".
12. M. S. Patterson, B. Chance, and B. C. Wilson, "Time resolved reflectance and transmittance for the non-invasive measurement of optical properties," *Appl. Opt.* 28, 2331–2336 (1989).
13. R. Cubeddu, A. Pifferi, P. Taroni, A. Torricelli, and G. Valentini, "Experimental test of theoretical models for time-resolved reflectance," *Med. Phys.* 23, 1625–1633 (1996).
14. Taroni, P., Pifferi, A., Salvagnini, E., Spinelli, L., Torricelli, A., Cubeddu, R. Seven-wavelength time-resolved optical mammography extending beyond 1000 nm for breast collagen quantification (2009) *Optics Express*, 17 (18), pp. 15932-15946.
15. J. R. Mourant, T. Fuselier, J. Boyer, T. M. Johnson, and I. J. Bigio, "Predictions and measurements of scattering and absorption over broad wavelength ranges in tissue phantoms," *Appl. Opt.* 36, 949–957 (1997).
16. Torricelli, A., Quaresima, V., Pifferi, A., Biscotti, G., Spinelli, L., Taroni, P., Ferrari, M., Cubeddu, R. Mapping of calf muscle oxygenation and haemoglobin content during dynamic plantar flexion exercise by multi-channel time-resolved near-infrared spectroscopy (2004) *Physics in Medicine and Biology*, 49 (5), pp. 685-699.